We are IntechOpen,
the world's leading publisher of
Open Access books
Built by scientists, for scientists

6,900
Open access books available

186,000
International authors and editors

200M
Downloads

Our authors are among the

154
Countries delivered to

TOP 1%
most cited scientists

12.2%
Contributors from top 500 universities

CLARIVATE ANALYTICS
BOOK CITATION INDEX
INDEXED

WEB OF SCIENCE™

Selection of our books indexed in the Book Citation Index
in Web of Science™ Core Collection (BKCI)

Interested in publishing with us?
Contact book.department@intechopen.com

2

Dynamic Modeling and Simulation of Stewart Platform

Zafer Bingul and Oguzhan Karahan
Mechatronics Engineering, Kocaeli University
Turkey

1. Introduction

Since a parallel structure is a closed kinematics chain, all legs are connected from the origin of the tool point by a parallel connection. This connection allows a higher precision and a higher velocity. Parallel kinematic manipulators have better performance compared to serial kinematic manipulators in terms of a high degree of accuracy, high speeds or accelerations and high stiffness. Therefore, they seem perfectly suitable for industrial high-speed applications, such as pick-and-place or micro and high-speed machining. They are used in many fields such as flight simulation systems, manufacturing and medical applications.

One of the most popular parallel manipulators is the general purpose 6 degree of freedom (DOF) Stewart Platform (SP) proposed by Stewart in 1965 as a flight simulator (Stewart, 1965). It consists of a top plate (moving platform), a base plate (fixed base), and six extensible legs connecting the top plate to the bottom plate. SP employing the same architecture of the Gough mechanism (Merlet, 1999) is the most studied type of parallel manipulators. This is also known as Gough–Stewart platforms in literature.

Complex kinematics and dynamics often lead to model simplifications decreasing the accuracy. In order to overcome this problem, accurate kinematic and dynamic identification is needed. The kinematic and dynamic modeling of SP is extremely complicated in comparison with serial robots. Typically, the robot kinematics can be divided into forward kinematics and inverse kinematics. For a parallel manipulator, inverse kinematics is straight forward and there is no complexity deriving the equations. However, forward kinematics of SP is very complicated and difficult to solve since it requires the solution of many non-linear equations. Moreover, the forward kinematic problem generally has more than one solution. As a result, most research papers concentrated on the forward kinematics of the parallel manipulators (Bonev and Ryu, 2000; Merlet, 2004; Harib and Srinivasan, 2003; Wang, 2007).

For the design and the control of the SP manipulators, the accurate dynamic model is very essential. The dynamic modeling of parallel manipulators is quite complicated because of their closed-loop structure, coupled relationship between system parameters, high nonlinearity in system dynamics and kinematic constraints. Robot dynamic modeling can be also divided into two topics: inverse and forward dynamic model. The inverse dynamic model is important for system control while the forward model is used for system simulation. To obtain the dynamic model of parallel manipulators, there are many valuable studies published by many researches in the literature. The dynamic analysis of parallel manipulators has been traditionally performed through several different methods such as

the Newton-Euler method, the Lagrange formulation, the principle of virtual work and the screw theory.

The Newton–Euler approach requires computation of all constraint forces and moments between the links. One of the important studies was presented by Dasgupta and Mruthyunjaya (1998) on dynamic formulation of the SP manipulator. In their study, the closed-form dynamic equations of the 6-UPS SP in the task-space and joint-space were derived using the Newton-Euler approach. The derived dynamic equations were implemented for inverse and forward dynamics of the Stewart Platform manipulator, and the simulation results showed that this formulation provided a complete modeling of the dynamics of SP. Moreover, it demonstrated the strength of the Newton-Euler approach as applied to parallel manipulators and pointed out an efficient way of deriving the dynamic equations through this formulation. This method was also used by Khalil and Ibrahim (2007). They presented a simple and general closed form solution for the inverse and forward dynamic models of parallel robots. The proposed method was applied on two parallel robots with different structures. Harib and Srinivasan (2003) performed kinematic and dynamic analysis of SP based machine structures with inverse and forward kinematics, singularity, inverse and forward dynamics including joint friction and actuator dynamics. The Newton-Euler formulation was used to derive the rigid body dynamic equations. Do and Yang (1988) and Reboulet and Berthomieu, (1991) presented the dynamic modeling of SP using Newton–Euler approach. They introduced some simplifications on the legs models. In addition to these works, others (Guo and Li, 2006; Carvalho and Ceccarelli, 2001; Riebe and Ulbrich, 2003) also used the Newton-Euler approach.

Another method of deriving the dynamics of the SP manipulator is the Lagrange formulation. This method is used to describe the dynamics of a mechanical system from the concepts of work and energy. Abdellatif and Heimann (2009) derived the explicit and detailed six-dimensional set of differential equations describing the inverse dynamics of non-redundant parallel kinematic manipulators with the 6 DOF. They demonstrated that the derivation of the explicit model was possible by using the Lagrangian formalism in a computationally efficient manner and without simplifications. Lee and Shah (1988) derived the inverse dynamic model in joint space of a 3-DOF in parallel actuated manipulator using Lagrangian approach. Moreover, they gave a numerical example of tracing a helical path to demonstrate the influence of the link dynamics on the actuating force required. Guo and Li (2006) derived the explicit compact closed-form dynamic equations of six DOF SP manipulators with prismatic actuators on the basic of the combination of the Newton-Euler method with the Lagrange formulation. In order to validate the proposed formulation, they studied numerical examples used in other references. The simulation results showed that it could be derived explicit dynamic equations in the task space for Stewart Platform manipulators by applying the combination of the Newton-Euler with the Lagrange formulation. Lebret and co-authors (1993) studied the dynamic equations of the Stewart Platform manipulator. The dynamics was given in step by step algorithm. Lin and Chen presented an efficient procedure for computer generation of symbolic modeling equations for the Stewart Platform manipulator. They used the Lagrange formulation for derivation of dynamic equations (Lin and Chen, 2008). The objective of the study was to develop a MATLAB-based efficient algorithm for computation of parallel link robot manipulator dynamic equations. Also, they proposed computer-torque control in order to verify the effectiveness of the dynamic equations. Lagrange's method was also used by others (Gregório and Parenti-Castelli, 2004; Beji and Pascal 1999; Liu et al., 1993).

For dynamic modeling of parallel manipulators, many approaches have been developed such as the principle of virtual work (Tsai, 2000, Wang and Gosselin, 1998; Geike and McPhee, 2003), screw teory (Gallardo et al., 2003), Kane's method (Liu et al., 2000; Meng et al., 2010) and recursive matrix method (Staicu and Zhang, 2008). Although the derived equations for the dynamics of parallel manipulators present different levels of complexity and computational loads, the results of the actuated forces/torques computed by different approaches are equivalent. The main goal of recent proposed approaches is to minimize the number of operations involved in the computation of the manipulator dynamics. It can be concluded that the dynamic equations of parallel manipulators theoretically have no trouble. Moreover, in fact, the focus of attention should be on the accuracy and computation efficiency of the model.

The aim of this paper is to present the work on dynamic formulation of a 6 DOF SP manipulator. The dynamical equations of the manipulator have been formulated by means of the Lagrangian method. The dynamic model included the rigid body dynamics of the mechanism as well as the dynamics of the actuators. The Jacobian matrix was derived in two different ways. Obtaining the accurate Jacobian matrix is very essential for accurate simulation model. Finally, the dynamic equations including rigid body and actuator dynamics were simulated in MATLAB-Simulink and verified on physical system.

This chapter is organized in the following manner. In Section 2, the kinematic analysis and Jacobian matrices are introduced. In Section 3, the dynamic equations of a 6 DOF SP manipulator are presented. In Section 4, dynamic simulations and the experimental results are given in detail. Finally, conclusions of this study are summarized.

2. Structure description and kinematic analysis

2.1 Structure description

The SP manipulator used in this study (Figure 1), is a six DOF parallel mechanism that consists of a rigid body moving plate, connected to a fixed base plate through six independent kinematics legs. These legs are identical kinematics chains, couple the moveable upper and the fixed lower platform by universal joints. Each leg contains a precision ball-screw assembly and a DC- motor. Thus, length of the legs is variable and they can be controlled separately to perform the motion of the moving platform.
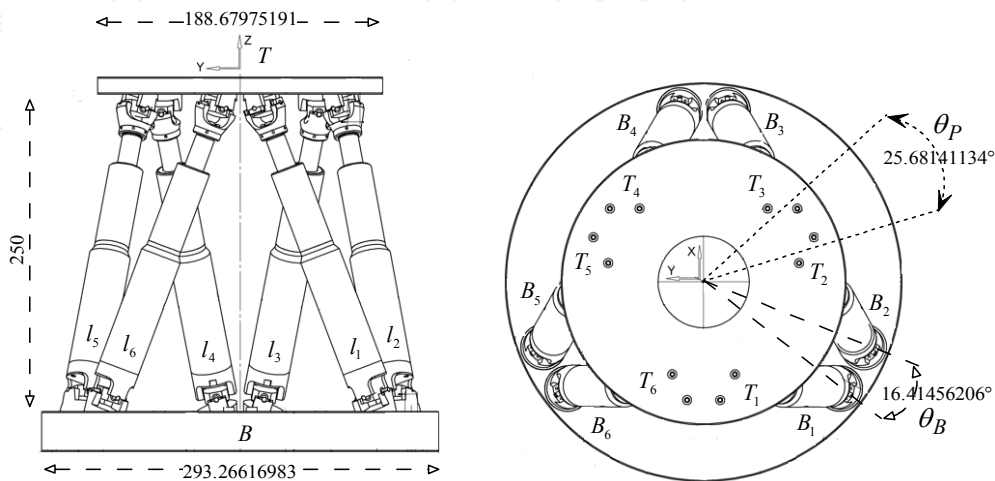

Fig. 1. Solid model of the SP manipulator

2.2 Inverse kinematics

To clearly describe the motion of the moving platform, the coordinate systems are illustrated in Figure 2. The coordinate system (B_{XYZ}) is attached to the fixed base and other coordinate system (T_{xyz}) is located at the center of mass of the moving platform. Points (B_i and T_i) are the connecting points to the base and moving platforms, respectively. These points are placed on fixed and moving platforms (Figure 2.a). Also, the separation angles between points (T_2 and T_3, T_4 and T_5, T_1 and T_6) are denoted by θ_p as shown in Figure 2.b. In a similar way, the separation angles between points (B_1 and B_2, B_3 and B_4, B_5 and B_6) are denoted by θ_b.

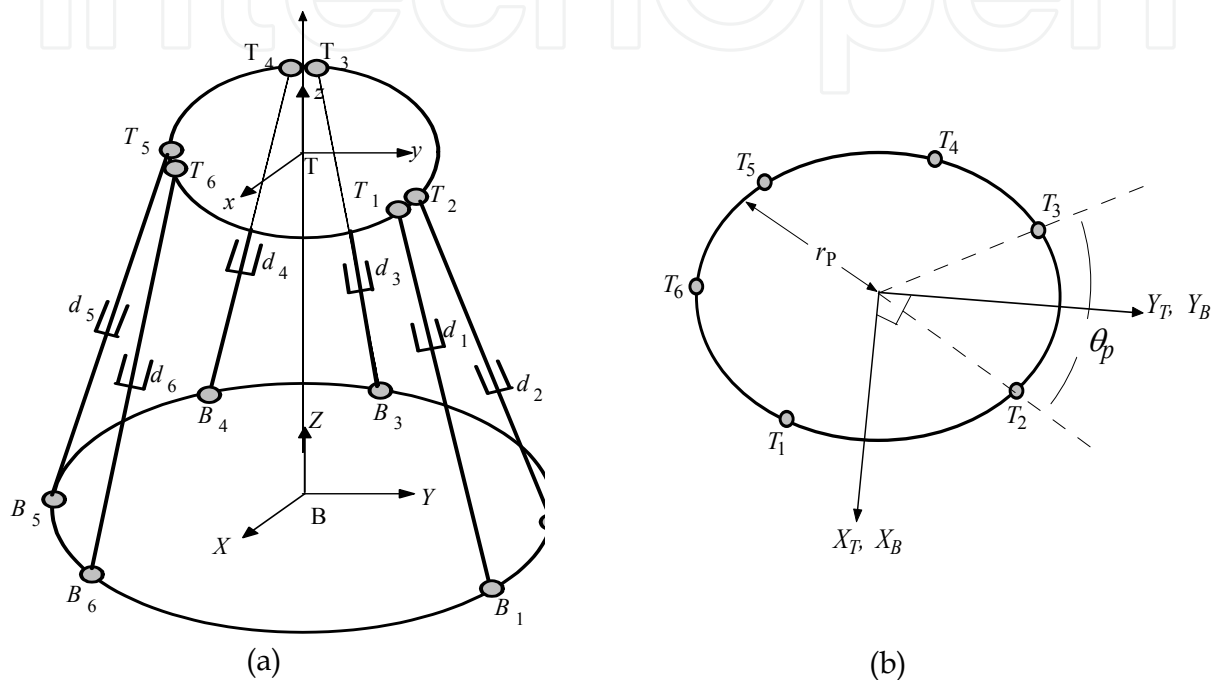(a)   (b)

Fig. 2. The schematic diagram of the SP manipulator

From Figure 2.b, the location of the ith attachment point (T_i) on the moving platform can be found (Equation 1). r_p and r_{base} are the radius of the moving platform and fixed base, respectively. By the using the same approach, the location of the ith attachment point (B_i) on the base platform can be also obtained from Equation 2.

$$GT_i = \begin{bmatrix} GT_{xi} \\ GT_{yi} \\ GT_{zi} \end{bmatrix} = \begin{bmatrix} r_p \cos(\lambda_i) \\ r_p \sin(\lambda_i) \\ 0 \end{bmatrix}, \quad \begin{aligned} \lambda_i &= \frac{i\pi}{3} - \frac{\theta_p}{2} & i &= 1,3,5 \\ \lambda_i &= \lambda_{i-1} + \theta_p & i &= 2,4,6 \end{aligned} \tag{1}$$

$$B_i = \begin{bmatrix} B_{xi} \\ B_{yi} \\ B_{zi} \end{bmatrix} = \begin{bmatrix} r_{base} \cos(\upsilon_i) \\ r_{base} \sin(\upsilon_i) \\ 0 \end{bmatrix}, \quad \begin{aligned} \upsilon_i &= \frac{i\pi}{3} - \frac{\theta_b}{2} & i &= 1,3,5 \\ \upsilon_i &= \upsilon_{i-1} + \theta_b & i &= 2,4,6 \end{aligned} \tag{2}$$

The pose of the moving platform can be described by a position vector, P and a rotation matrix, $^B R_T$. The rotation matrix is defined by the roll, pitch and yaw angles, namely, a

rotation of α about the fixed *x-axis*, $R_X(\alpha)$, followed by a rotaion of β about the fixed *y-axis*, $R_Y(\beta)$ and a rotaion of γ about the fixed *z-axis*, $R_Z(\gamma)$. In this way, the rotation matrix of the moving platform with respect to the base platform coordinate system is obtained. The position vector *P* denotes the translation vector of the origin of the moving platform with respect to the base platform. Thus, the rotation matrix and the position vector are given as the following.

$$
\begin{aligned}
^{B}R_T = R_Z(\gamma)R_Y(\beta)R_X(\alpha) &= \begin{bmatrix} r_{11} & r_{12} & r_{13} \\ r_{21} & r_{22} & r_{23} \\ r_{31} & r_{32} & r_{33} \end{bmatrix} \\
&= \begin{bmatrix} \cos\beta\cos\gamma & \cos\gamma\sin\alpha\sin\beta - \cos\alpha\sin\gamma & \sin\alpha\sin\gamma + \cos\alpha\cos\gamma\sin\beta \\ \cos\beta\sin\gamma & \cos\alpha\cos\gamma + \sin\alpha\sin\beta\sin\gamma & \cos\alpha\sin\beta\sin\gamma - \cos\gamma\sin\alpha \\ -\sin\beta & \cos\beta\sin\alpha & \cos\alpha\cos\beta \end{bmatrix}
\end{aligned} \tag{3}
$$

$$
P = \begin{bmatrix} P_x & P_y & P_z \end{bmatrix}^T \tag{4}
$$

Referring back to Figure 2, the above vectors GT_i and B_i are chosen as the position vector. The vector L_i of the link *i* is simply obtained as

$$
L_i = R_{XYZ}GT_i + P - B_i \qquad i=1,2,\dots,6. \tag{5}
$$

When the position and orientation of the moving platform $X_{p-o} = \begin{bmatrix} P_x & P_y & P_z & \alpha & \beta & \gamma \end{bmatrix}^T$ are given, the length of each leg is computed as the following.

$$
\begin{aligned}
l_i^2 &= \left(P_x - B_{xi} + GT_{xi}r_{11} + GT_{yi}r_{12} \right)^2 \\
&+ \left(P_y - B_{yi} + GT_{xi}r_{21} + GT_{yi}r_{22} \right)^2 + \left(P_z + GT_{xi}r_{31} + GT_{yi}r_{32} \right)^2
\end{aligned} \tag{6}
$$

The actuator length is $l_i = \|L_i\|$.

2.3 Jacobian matrix

The Jacobian matrix relates the velocities of the active joints (actuators) to the generalized velocity of the moving platform. For the parallel manipulators, the commonly used expression of the Jacobian matrix is given as the following.

$$
\dot{L} = J\dot{X} \tag{7}
$$

where $\dot{L}$ and $\dot{X}$ are the velocities of the leg and the moving platform, respectively. In this work, two different derivations of the Jacobian matrix are developed. The first derivation is made using the general expression of the Jacobian matrix given in Equation 7. It can be rewritten to see the relationship between the actuator velocities, $\dot{L}$ and the generalized velocity of the moving platform ($\dot{X}_{p-0}$) as the following

$$
\dot{L} = J_A \dot{X}_{p-0} = J_{IA} \vec{V}_{T_J} \tag{8}
$$

The generalized velocity of the moving platform is below:

$$\vec{V}_{T_j} = J_{IIA} \, \dot{X}_{p-o} \tag{9}$$

where $\vec{V}_{T_j}$ is the velocity of the platform connection point of the leg. Figure 3 shows a schematic view of one of the six legs of the SP manipulator.
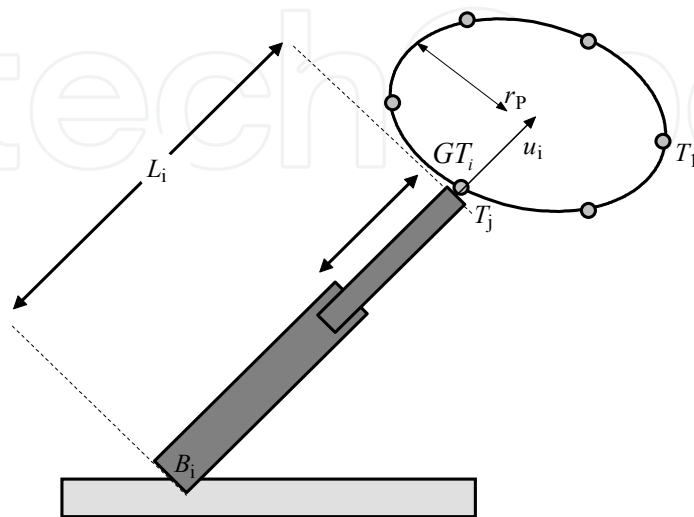

Fig. 3. Schematic view of the ith leg of the parallel manipulator

Now combining Equation 8 and Equation 9 gives

$$\dot{L} = J_A \, \dot{X}_{p-o} = J_{IA} \, J_{IIA} \, \dot{X}_{p-o} \tag{10}$$

The first Jacobian matrix in the equation above is

$$J_{IA} = \begin{bmatrix} \vec{u}_1^T & \cdots & \cdots & \cdots & \cdots & 0 \\ 0 & \vec{u}_2^T & \cdots & \cdots & \cdots & 0 \\ 0 & \cdots & \vec{u}_3^T & \cdots & \cdots & 0 \\ 0 & \cdots & \cdots & \vec{u}_4^T & \cdots & 0 \\ 0 & \cdots & \cdots & \cdots & \vec{u}_5^T & 0 \\ 0 & \cdots & \cdots & \cdots & \cdots & \vec{u}_6^T \end{bmatrix}_{6x18} \tag{11}$$

where u_i is the unit vector along the axis of the prismatic joint of link i (Figure 3). It can be obtained as follows

$$\vec{u}_i = \frac{B_i T_j}{|L_i|} = \frac{L_i}{l_i} \, , \begin{cases} j = \dfrac{i+1}{2} & \text{if } i \text{ is odd} \\[2em] j = \dfrac{i}{2} & \text{if } i \text{ is even} \end{cases} \tag{12}$$

The second Jacobian matrix in Equation 10 is calculated as the following.

$$
J_{IIA} = \begin{bmatrix} I_{3x3} & R_Y(\beta)S(X)R_X(\alpha)R_Z(\gamma)GT_1 & S(Y)R_Y(\beta)R_X(\alpha)R_Z(\gamma)GT_1 & R_Y(\beta)R_X(\alpha)S(Z)R_Z(\gamma)GT_1 \\ \vdots & \vdots & \vdots & \vdots \\ \vdots & \vdots & \vdots & \vdots \\ \vdots & \vdots & \vdots & \vdots \\ \vdots & \vdots & \vdots & \vdots \\ I_{3x3} & R_Y(\beta)S(X)R_X(\alpha)R_Z(\gamma)GT_6 & S(Y)R_Y(\beta)R_X(\alpha)R_Z(\gamma)GT_6 & R_Y(\beta)R_X(\alpha)S(Z)R_Z(\gamma)GT_6 \end{bmatrix}_{18x6} \tag{13}
$$

where I_{3x3} denotes the 3x3 identity matrix and S designates the 3x3 screw symmetric matrix associated with the vector $a = \begin{bmatrix} a_x & a_y & a_z \end{bmatrix}^T$,

$$
S = \begin{bmatrix} 0 & -a_z & a_y \\ a_z & 0 & -a_x \\ -a_y & a_x & 0 \end{bmatrix} \tag{14}
$$

The first proposed Jacobian matrix of the SP manipulator is defined as

$$
J_A = J_{IA} J_{IIA} \tag{15}
$$

The second proposed Jacobian matrix of the SP manipulator is defined as

$$
J_B = J_{IB} J_{IIB} \tag{16}
$$

Given $GT_i = \begin{bmatrix} GT_{xi} & GT_{yi} & GT_{zi} \end{bmatrix}^T$, T_j on the moving platform with reference to the base coordinate system (B_{XYZ}) is obtained as

$$
T_j = \begin{bmatrix} P_x & P_y & P_z \end{bmatrix}^T + {}^B R_T GT_i = x + {}^B R_T GT_i \tag{17}
$$

The velocity of the attachment point T_j is obtained by differentiating Equation 17 with respect to time

$$
\vec{V}_{T_j} = \begin{bmatrix} \dot{P}_x & \dot{P}_y & \dot{P}_z \end{bmatrix}^T + \omega \times {}^B R_T GT_i = \dot{x} + \omega \times {}^B R_T GT_i \tag{18}
$$

where $\omega = (\omega_x, \omega_y, \omega_z)$ is angular velocity of the moving platform with reference to the base platform.

$$
\omega = \begin{bmatrix} \omega_x \\ \omega_y \\ \omega_z \end{bmatrix} = \begin{bmatrix} \cos\beta & 0 & 0 \\ 0 & 1 & -\sin\alpha \\ -\sin\beta & 0 & \cos\alpha \end{bmatrix} = \begin{bmatrix} \dot{\alpha} \\ \dot{\beta} \\ \dot{\gamma} \end{bmatrix} \tag{19}
$$

Since the projection of the velocity vector ($\dot{T}_j$) on the axis of the prismatic joint of link i produces the extension rate of link i, the velocity of the active joint ($\dot{L}_i$) is computed from

$$
\dot{L}_i = \vec{V}_{T_j} \vec{u}_i = \begin{bmatrix} \dot{P}_x & \dot{P}_y & \dot{P}_z \end{bmatrix}^T \cdot \vec{u}_i + \omega \times \left({}^B R_T GT_i \right) \cdot \vec{u}_i = \dot{x} \cdot \vec{u}_i + \omega \times \left({}^B R_T GT_i \right) \cdot \vec{u}_i \tag{20}
$$

Equation 20 is rewritten in matrix format as follows.

$$\dot{L}_i = J_B \begin{bmatrix} \dot{x} \\ \omega \end{bmatrix} = J_B \, \dot{X}_{p-o} = J_{IB} \, J_{IIB} \, \dot{X}_{p-o} \tag{21}$$

The first Jacobian matrix is

$$J_{IB} = \begin{bmatrix} u_{x1} & u_{y1} & u_{z1} & \left({}^B R_T G T_1 \, x \, \vec{u}_1 \right)^T \\ \vdots & \vdots & \vdots & \vdots \\ u_{x6} & u_{y6} & u_{z6} & \left({}^B R_T G T_6 \, x \, \vec{u}_6 \right)^T \end{bmatrix}_{6x6} \tag{22}$$

The second Jacobian matrix is

$$J_{IIB} = \begin{bmatrix} 1 & 0 & 0 & 0 & 0 & 0 \\ 0 & 1 & 0 & 0 & 0 & 0 \\ 0 & 0 & 1 & 0 & 0 & 0 \\ 0 & 0 & 0 & \cos\beta & 0 & 0 \\ 0 & 0 & 0 & 0 & 1 & -\sin\alpha \\ 0 & 0 & 0 & -\sin\beta & 0 & \cos\alpha \end{bmatrix}_{6x6} \tag{23}$$

3. Dynamic modeling

The dynamic analysis of the SP manipulator is always difficult in comparison with the serial manipulator because of the existence of several kinematic chains all connected by the moving platform. Several methods were used to describe the problem and obtain the dynamic modeling of the manipulator. In the literature, there is still no consensus on which formulation is the best to describe the dynamics of the manipulator. Lagrange formulation was used in this work since it provides a well analytical and orderly structure.

In order to derive the dynamic equations of the SP manipulator, the whole system is separated into two parts: the moving platform and the legs. The kinetic and potential energies for both of these parts are computed and then the dynamic equations are derived using these energies.

3.1 Kinetic and potential energies of the moving platform

The kinetic energy of the moving platform is a summation of two motion energies since the moving platform has translation and rotation about three orthogonal axes, (*XYZ*). The first one is translation energy occurring because of the translation motion of the center of mass of the moving platform. The translation energy is defined by

$$K_{up(trans)} = \frac{1}{2} m_{up} \left(\dot{P}_X^2 + \dot{P}_Y^2 + \dot{P}_Z^2 \right) \tag{24}$$

where m_{up} is the moving platform mass. For rotational motion of the moving platform around its center of mass, rotational kinetic energy can be written as

$$K_{up(rot)} = \frac{1}{2} \vec{\Omega}_{up(mf)}^T I_{(mf)} \vec{\Omega}_{up(mf)} \tag{25}$$

where $I_{(mf)}$ and $\vec{\Omega}_{up(mf)}$ are the rotational inertia mass and the angular velocity of the moving platform, respectively. They are given as

$$I_{(mf)} = \begin{bmatrix} I_X & 0 & 0 \\ 0 & I_Y & 0 \\ 0 & 0 & I_Z \end{bmatrix} \tag{26}$$

$$\vec{\Omega}_{up(mf)} = R_Z(\gamma)^T R_X(\alpha)^T R_Y(\beta)^T \vec{\Omega}_{up(ff)} \tag{27}$$

where $\vec{\Omega}_{up(ff)}$ denotes the angular velocity of the moving platform with respect to the base frame. Given the definition of the angles α, β and γ , the angular velocity, $\vec{\Omega}_{up(ff)}$ is

$$
\begin{aligned}
\vec{\Omega}_{up(ff)} &= \dot{\alpha} R_Y(\beta)\vec{X} + \dot{\beta}\vec{Y} + \dot{\gamma} R_X(\alpha)R_Z(\gamma)\vec{Z} \\
&= \left(\begin{bmatrix} \cos\beta & 0 & \sin\beta \\ 0 & 1 & 0 \\ -\sin\beta & 0 & \cos\beta \end{bmatrix} \begin{bmatrix} 1 & 0 & 0 \\ 0 & 0 & 0 \\ 0 & 0 & 0 \end{bmatrix} + \begin{bmatrix} 0 & 0 & 0 \\ 0 & 1 & 0 \\ 0 & 0 & 0 \end{bmatrix} \right.
\end{aligned} \tag{28}
$$

$$
\left. + \begin{bmatrix} 1 & 0 & 0 \\ 0 & \cos\alpha & -\sin\alpha \\ 0 & \sin\alpha & \cos\alpha \end{bmatrix} \begin{bmatrix} \cos\gamma & -\sin\gamma & 0 \\ \sin\gamma & \cos\gamma & 0 \\ 0 & 0 & 1 \end{bmatrix} \begin{bmatrix} 0 & 0 & 0 \\ 0 & 0 & 0 \\ 0 & 0 & 1 \end{bmatrix} \right) \begin{bmatrix} \dot{\alpha} \\ \dot{\beta} \\ \dot{\gamma} \end{bmatrix} = \begin{bmatrix} \cos\beta & 0 & 0 \\ 0 & 1 & -\sin\alpha \\ -\sin\beta & 0 & \cos\alpha \end{bmatrix} \begin{bmatrix} \dot{\alpha} \\ \dot{\beta} \\ \dot{\gamma} \end{bmatrix}
$$

In the moving platform coordinate system, the angular velocity of the moving platform given in Equation 27 is calculated as

$$\vec{\Omega}_{up(mf)} = \begin{bmatrix} c\gamma & c\alpha s\gamma & -c\alpha c\gamma s\beta - c\alpha s\alpha s\gamma + c\alpha c\beta s\alpha s\gamma \\ -s\gamma & c\alpha c\gamma & -c\alpha c\gamma s\alpha + c\alpha s\beta s\gamma + c\alpha c\beta s\alpha c\gamma \\ 0 & -s\alpha & s^2\alpha + c^2\alpha c\beta \end{bmatrix} \begin{bmatrix} \dot{\alpha} \\ \dot{\beta} \\ \dot{\gamma} \end{bmatrix} \tag{29}$$

where $s(\cdot) = \sin(\cdot)$ and $c(\cdot) = \cos(\cdot)$. As a result, the total kinetic energy of the moving platform in a compact form is given by

$$
\begin{aligned}
K_{up} &= K_{up(trans)} + K_{up(rot)} = \frac{1}{2} m_{up} \left(\dot{P}_X^2 + \dot{P}_Y^2 + \dot{P}_Z^2 \right) + \frac{1}{2} \vec{\Omega}_{up(mf)}^T I_{(mf)} \vec{\Omega}_{up(mf)} \\
&= \frac{1}{2} \dot{X}_{P-O}^T \cdot M_{up}(X_{P-O}) \cdot \dot{X}_{P-O} = \frac{1}{2} \begin{bmatrix} \dot{P}_X & \dot{P}_Y & \dot{P}_Z & \dot{\alpha} & \dot{\beta} & \dot{\gamma} \end{bmatrix} M_{up} \begin{bmatrix} \dot{P}_X \\ \dot{P}_Y \\ \dot{P}_Z \\ \dot{\alpha} \\ \dot{\beta} \\ \dot{\gamma} \end{bmatrix}
\end{aligned} \tag{30}
$$

where M_{up} is the 6x6 mass diagonal matrix of the moving platform. Also, potential energy of the moving platform is

$$P_{up} = m_{up}gP_ZX_{P-O} = \begin{bmatrix} 0 & 0 & m_{up}g & 0 & 0 & 0 \end{bmatrix} \begin{bmatrix} P_X \\ P_Y \\ P_Z \\ \alpha \\ \beta \\ \gamma \end{bmatrix} \quad (31)$$

where g is the gravity.

3.2 Kinetic and potential energies of the legs

Each leg consists of two parts: the moving part and the fixed part (Figure 4). The lower fixed part of the leg is connected to the base platform through a universal joint, whereas the upper moving part is connected to the moving platform through a universal joint.
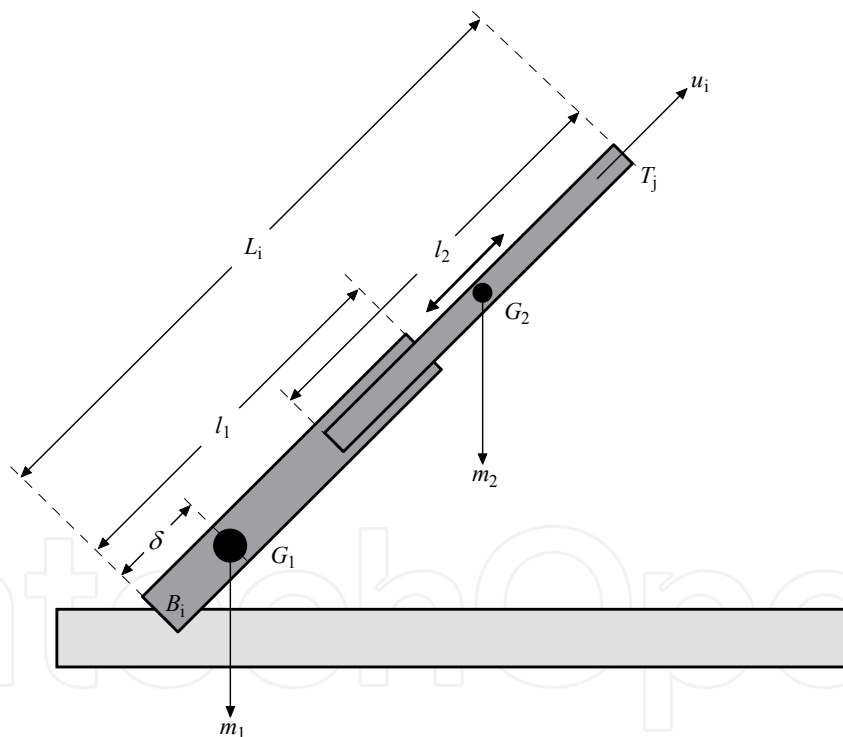
Fig. 4. Leg of the SP manipulator

As shown in the figure above, the center of mass, G_i for each part of the leg ($Leg_i\ i = 1...6$) is considered. G_{1i} denotes the center of mass of the fixed part. l_1 and m_1 are the length and the mass of the fixed part, respectively and δ is the distance between B_i and G_i. For the moving part of the leg, G_{2i} denotes its center of mass. l_2 and m_2 are the length and mass of the part, respectively.

The length of the leg is assumed to be constant. The rotational kinetic energy caused by the rotation around the fixed point B_i as shown in Figure 4 is given by

$$K_{Li(rot)} = \frac{1}{2}(m_1 + m_2)\left[h_i\left(\vec{V}_{T_j}^T\vec{V}_{T_j} - \vec{V}_{T_j}^T\vec{u}_i\vec{u}_i^T\vec{V}_{T_j}\right)\right], \quad \begin{cases} j = \dfrac{i+1}{2} & \text{if } i \text{ is odd} \\ j = \dfrac{i}{2} & \text{if } i \text{ is even} \end{cases} \tag{32}$$

where

$$h_i = \left(\frac{\hat{I}}{L_i} + \frac{m_2}{m_1 + m_2}\right)^2, \hat{I} = \frac{1}{m_1 + m_2}\left(\delta m_1 l_1 - \frac{1}{2}m_2 l_2\right) \tag{33}$$

Moreover, the translation kinetic energy due to the translation motion of the leg is computed from

$$K_{Li(trans)} = \frac{1}{2}(m_1 + m_2)\left[\left(\frac{m_2}{m_1 + m_2}\right)^2 \vec{V}_{T_j}^T\vec{u}_i\vec{u}_i^T\vec{V}_{T_j}\right] \tag{34}$$

Therefore, the total kinetic energy of the leg L_i is calculated as the following.

$$K_{Li} = K_{Li(rot)} + K_{Li(trans)} = \frac{1}{2}(m_1 + m_2)\left[\vec{V}_{T_j}^T h_i \vec{V}_{T_j} - \dot{L}_i k_i \dot{L}_i\right] \tag{35}$$

where

$$k_i = \frac{\hat{I}}{L_i}\left(\frac{\hat{I}}{L_i} + \frac{m_2}{m_1 + m_2}\right) = h_i - \left(\frac{m_2}{m_1 + m_2}\right)^2 \tag{36}$$

Remember that $\vec{u}_i$ is the unit vector along the axis of the leg (L_i). By using this vector, the velocity of the leg can be calculated by $\dot{L}_i = \vec{V}_{T_j}\vec{u}_i$.

As a result, the compact expression for the kinetic energy of the six legs can be written as

$$K_{Legs} = \sum_{i=1}^{6}K_{Li} = \frac{1}{2}\dot{X}_{P-O}^T \cdot M_{Legs}\left(X_{P-O}\right)\cdot\dot{X}_{P-O} \tag{37}$$

Total potential energy of the legs can be defined as

$$P_{Legs} = (m_1 + m_2)g\sum_{i=1}^{3}\left[\hat{I}\left(\frac{1}{L_{2i}} + \frac{1}{L_{2i-1}}\right) + \frac{2m_2}{m_1 + m_2}\right]\left(p_z + Z_{T_j}\right) \tag{38}$$

where

$$Z_{T_j} = \begin{bmatrix}0\\0\\1\end{bmatrix}^T R_Z(\gamma)^T R_X(\alpha)^T R_Y(\beta)^T GT_j, \quad \begin{cases} j = \dfrac{i+1}{2} & \text{if } i \text{ is odd} \\ j = \dfrac{i}{2} & \text{if } i \text{ is even} \end{cases} \tag{39}$$

3.3 Dynamic equations

In this subsection, the Lagrange formulation is used to derive the dynamic modeling of the SP manipulator. Considering q and τ as the corresponding generalized coordinates and generalized forces, respectively, the general classical equations of the motion can be obtained from the Lagrange formulation:

$$\frac{d}{dt}\frac{dL}{d\dot{q}} - \frac{\partial L}{\partial q} = \frac{d}{dt}\left(\frac{\partial K(q,\dot{q})}{\partial \dot{q}}\right) - \frac{\partial K(q,\dot{q})}{\partial q} + \frac{\partial P(q)}{\partial q} = \tau \qquad (40)$$

where $K(q,\dot{q})$ is the kinetic energy, and $P(q)$ is the potential energy.

Generalized coordinates q is replaced with Cartesian coordinates (X_{p-o}). The dynamic equation derived from Equation 40 can be written as

$$J^T(X_{P-O})F = M(X_{P-O})\ddot{X}_{P-O} + V_m(X_{P-O}, \dot{X}_{P-O})\dot{X}_{P-O} + G(X_{P-O}) \qquad (41)$$

where $F = \begin{bmatrix} f_1 & f_2 & f_3 & f_4 & f_5 & f_6 \end{bmatrix}$, f_i is the force applied by the actuator of leg i in the direction $\vec{u}_i$ and J is the Jacobian matrix. Since the platform is divided into two parts (the moving platform and the legs), inertia, Coriolis-Centrifugal and gravity matrix in Equation 41 are summation of two matrix. Each of these matrices is computed using by two different Jacobian matrices.

$$^A M(X_{p-o}) = M_{up} + {}^A M_{Legs}, \qquad {}^B M(X_{p-o}) = M_{up} + {}^B M_{Legs} \qquad (42)$$

$$^A V_m(X_{p-o}, \dot{X}_{p-o}) = V_{mup} + {}^A V_{mLegs}, \qquad {}^B V_m(X_{p-o}, \dot{X}_{p-o}) = V_{mup} + {}^B V_{mLegs} \qquad (43)$$

$$^A G(X_{p-o}) = G_{up} + {}^A G_{Legs}, \qquad {}^B G(X_{p-o}) = G_{up} + {}^B G_{Legs} \qquad (44)$$

where M_{up} obtained from Equation 30, $^A M_{Legs}$ and $^B M_{Legs}$ obtained from Equation 37 are the inertia matrix of the moving platform and legs, respectively. V_{mup}, $^A V_{mLegs}$ and $^B V_{mLegs}$ are Coriolis-Centrifugal matrix of the moving platform and legs, respectively. G_{up}, $^A G_{Legs}$ and $^B G_{Legs}$ are the gravity matrix of the moving platform and legs, respectively. V_{mup}, $^A V_{mLegs}$ and $^B V_{mLegs}$ are defined as follows:

$$V_{mup(i,j)} = \frac{1}{2}\sum_{k=1}^{6}\left(\frac{\partial M_{up}(k,j)}{\partial X_{p-o}(i)} + \frac{\partial M_{up}(k,i)}{\partial X_{p-o}(j)} - \frac{\partial M_{up}(i,j)}{\partial X_{p-o}(k)}\right)\dot{X}_{p-o}(k) \qquad (45)$$

$$^A V_{Legs(i,j)} = \frac{1}{2}\sum_{k=1}^{6}\left(\frac{\partial {}^A M_{Legs}(k,j)}{\partial X_{p-o}(i)} + \frac{\partial {}^A M_{Legs}(k,i)}{\partial X_{p-o}(j)} - \frac{\partial {}^A M_{Legs}(i,j)}{\partial X_{p-o}(k)}\right)\dot{X}_{p-o}(k) \qquad (46)$$

$$^B V_{Legs(i,j)} = \frac{1}{2}\sum_{k=1}^{6}\left(\frac{\partial {}^B M_{Legs}(k,j)}{\partial X_{p-o}(i)} + \frac{\partial {}^B M_{Legs}(k,i)}{\partial X_{p-o}(j)} - \frac{\partial {}^B M_{Legs}(i,j)}{\partial X_{p-o}(k)}\right)\dot{X}_{p-o}(k) \qquad (47)$$

Finally, the gravity matrix can be obtained from the equations below.

$$G_{up}(k) = \frac{\partial P_{up}(X_{p-o})}{\partial X_{p-o}(k)} \tag{48}$$

$$^A G_{Legs}(k) = \frac{\partial\, ^A P_{Legs}(X_{p-o})}{\partial X_{p-o}(k)}$$

$$= (m_1 + m_2)g\sum_{i=1}^{3}\left[\hat{I}\left[\frac{1}{^A L_{2i}^2}\left(\frac{\partial\, ^A L_{2i}}{\partial X_{p-o}(k)}\right) + \frac{1}{^A L_{2i-1}^2}\left(\frac{\partial\, ^A L_{2i-1}}{\partial X_{p-o}(k)}\right)\right]\right]\left(p_z + Z_{T_i}\right) \tag{49}$$

$$+ (m_1 + m_2)g\sum_{i=1}^{3}\left[\hat{I}\left(\frac{1}{^A L_{2i}} + \frac{1}{^A L_{2i-1}}\right) + \frac{2m_2}{(m_1 + m_2)}\right]\left(p_z + Z_{T_i}\right)$$

$$^B G_{Legs}(k) = \frac{\partial\, ^B P_{Legs}(X_{p-o})}{\partial X_{p-o}(k)}$$

$$= (m_1 + m_2)g\sum_{i=1}^{3}\left[\hat{I}\left[\frac{1}{^B L_{2i}^2}\left(\frac{\partial\, ^B L_{2i}}{\partial X_{p-o}(k)}\right) + \frac{1}{^B L_{2i-1}^2}\left(\frac{\partial\, ^B L_{2i-1}}{\partial X_{p-o}(k)}\right)\right]\right]\left(p_z + Z_{T_i}\right) \tag{50}$$

$$+ (m_1 + m_2)g\sum_{i=1}^{3}\left[\hat{I}\left(\frac{1}{^B L_{2i}} + \frac{1}{^B L_{2i-1}}\right) + \frac{2m_2}{(m_1 + m_2)}\right]\left(p_z + Z_{T_i}\right)$$

In equation 49 and 50, the expression of $\left(\dfrac{\partial L_n}{\partial X_{p-o}(k)}\right)$ is needed to compute. This can be obtained using with the Jacobian matrices (J_A and J_B) as follows:

$$\frac{\partial\, ^A L_n}{\partial X_{p-o}(k)} = \sum_{m=1}^{9} J_{IA_{nm}}\, J_{IIA_{mk}}, \qquad \frac{\partial\, ^B L_n}{\partial X_{p-o}(k)} = \sum_{m=1}^{9} J_{IB_{nm}}\, J_{IIB_{mk}} \tag{51}$$

3.4 Actuator dynamics
6 identical motor-ball-screw drives are used in SP. Dynamic equation of SP with actuator dynamics can be written in matrix form as

$$\tau_m = M_a\ddot{L} + N_a\dot{L} + K_a F \tag{52}$$

$$M_a = \frac{2\pi}{np}\left(J_s + n^2 J_m\right)I_{6x6} \tag{53}$$

$$N_a = \frac{2\pi}{np}\left(b_s + n^2 b_m\right)I_{6x6} \tag{54}$$

$$K_a = \frac{p}{n2\pi}I_{6x6} \tag{55}$$

where M_a , N_a and K_a are the inertia matrix, viscous damping coefficient matrix and gain matrix of the actuator, respectively. Also, J_s and J_m are the mass moment of inertia of the ball-screw and motor, b_s and b_m are the viscous damping coefficient of the ball-screw and motor, p and n are the pitch of the ball-screw and the gear ratio. τ_m and F are the vectors of motor torques and the forces applied by the actuators.

The electrical dynamics of the actuator can be described by the following equations.

$$\tau_m = K_t i \tag{56}$$

$$V = L\frac{di}{dt} + R i + K_b\dot{\theta}_m \tag{57}$$

where K_t , L , R and K_b are the torque constant, the rotor inductance, terminal resistance and back-emf constant of the actuators, respectively. V and i are the motor voltage and motor current , respectively. The angular velocity of the motor is given as

$$\dot{\theta}_m = \frac{2\pi n}{p}\dot{L} \tag{58}$$

Since the dynamics of the platform is derived in the moving platform coordinates (Cartesian space, X_{p-o}), Equation 52 can be generally expressed in Cartesian space as the follows.

$$\tau_m = \bar{M}_c(X)\ddot{X} + \bar{N}_c(X)\dot{X} + \bar{G}_c(X) \tag{59}$$

The terms in the equation above are obtained from joint space terms and the Jacobian matrix.

$$^A\bar{M}_c(X) = K_a\left(J_A\right)^{-T}{}^A M(X_{p-o}) + M_a J_A \tag{60}$$

$$^B\bar{M}_c(X) = K_a\left(J_B\right)^{-T}{}^B M(X_{p-o}) + M_a J_B \tag{61}$$

$$^A\bar{N}_c(X) = K_a\left(J_A\right)^{-T}{}^A N(X_{p-o},\dot{X}_{p-o}) + N_a J_A + M_a \dot{J}_A \tag{62}$$

$$^B\bar{N}_c(X) = K_a\left(J_B\right)^{-T}{}^B N(X_{p-o},\dot{X}_{p-o}) + N_a J_B + M_a \dot{J}_B \tag{63}$$

$$^A\bar{G}_c(X) = K_a\left(J_A\right)^{-T}{}^A G(X_{p-o}) \tag{64}$$

$$^B\bar{G}_c(X) = K_a\left(J_B\right)^{-T}{}^B G(X_{p-o}) \tag{65}$$

Figure 5 shows the simulation block diagram of the Stewart Platform manipulator including the actuator dynamics (Equation 56, 57, 58 and 59). In order to model the platform dynamics without using forward kinematics, the block diagram is developed below.
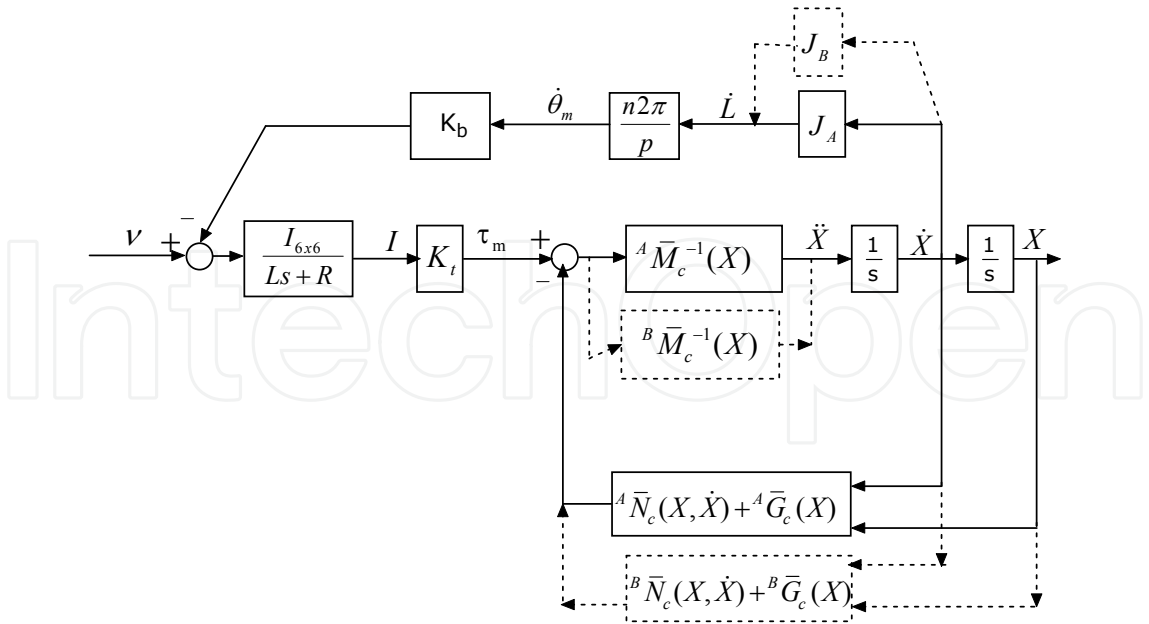
Fig. 5. Simulation block diagram for SP dynamics

4. Results

4.1 Experimental setup and simulation blocks

Figure 6 shows the Stewart Platform manipulator used in the experiments. It is constructed from two main bodies (top and base plates), six linear motors, controller, space mouse, accelerometer, gyroscope, force/torque sensor, power supply, emergency stop circuit and interface board as shown in the figure. Inverse kinematics and control algorithm of SP are embedded in MATLAB/Simulink module. Moreover, controller board like the space DS1103owning real-time interface implementation software to generate and then download the real time code to specific space board is used, and it is fully programmable from MATLAB/Simulink environment. Thus, it is possible for the user to observe the real process and collect the data from encoders for each leg while the experiment is in progress.

Fig. 6. SP manipulator used in experiments

To demonstrate the effectiveness and the validation of the two dynamic models of the SP manipulator including the actuator dynamics, experimental tests are performed on the manipulator.

The first Simulink model ("*Desired*" block) as shown in Figure 7 is used for the inverse kinematic solution for a given $X_{p-o} = \begin{bmatrix} P_x & P_y & P_z & \alpha & \beta & \gamma \end{bmatrix}^T$. Thus, the reference lengths of the legs are obtained from this block. Figure 8 shows the forward dynamics Simulink block (Jacobian matrix and its derivative, motor torques, the position and velocity of the moving platform, etc.). Figure 9 shows the developed Simulink model for the actual lengths of the legs. This block is designed using the following equation.

$$\ddot{L}_i = \dot{J}\, \dot{X}_{P-O} + J\, \ddot{X}_{P-O} \tag{66}$$
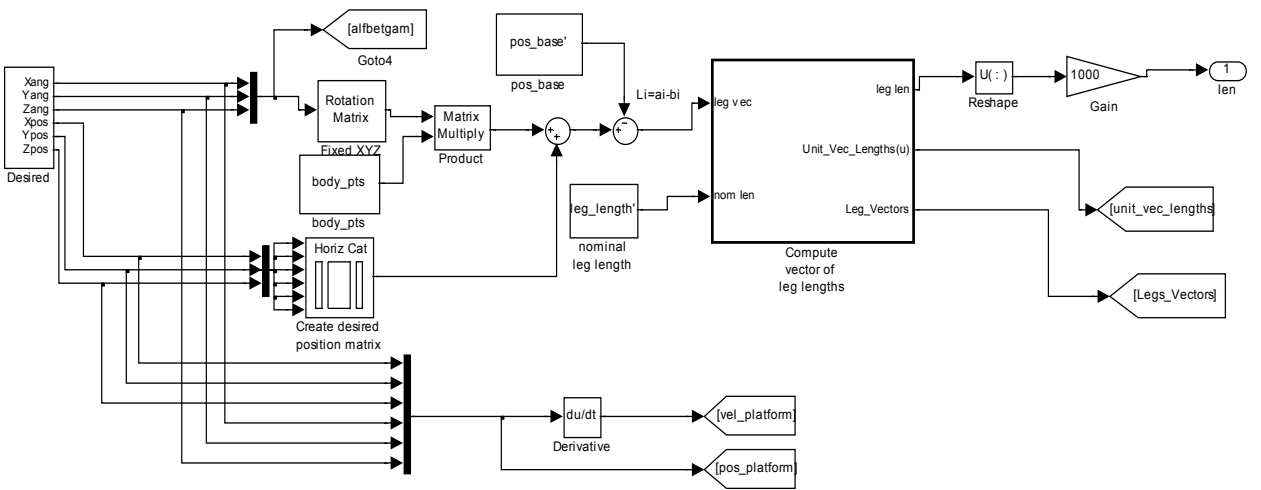
Fig. 7. Inverse kinematic solution Simulink model, "*Leg_Trajectory*"block
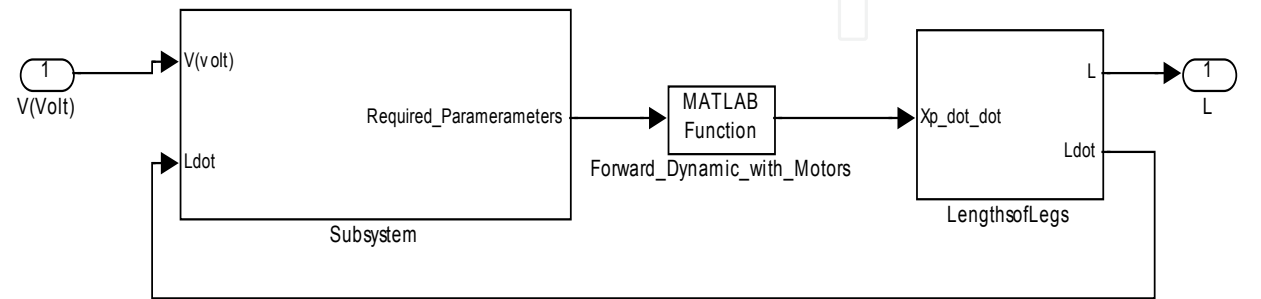
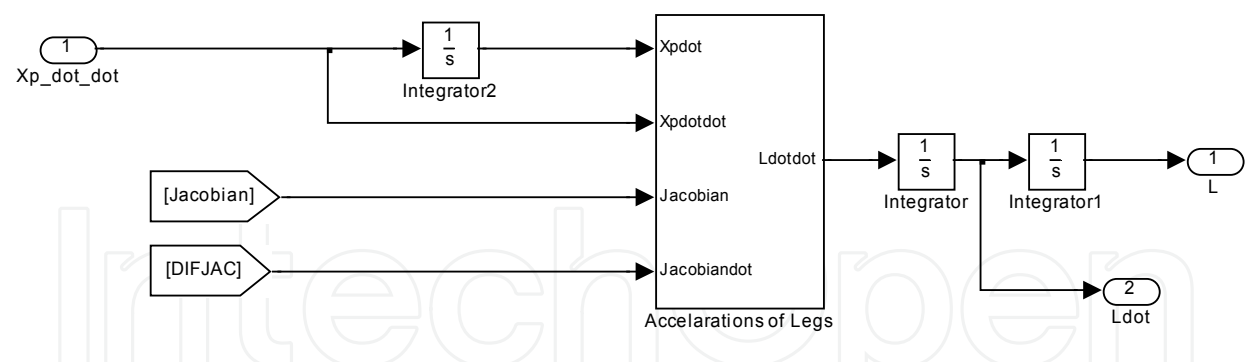Fig. 8. The Simulink model of the forward dynamics, "*Stewart_Platform_Dynamics*'' block

Fig. 9. The leg Simulink model, "*LengthofLegs*"block

To examine trajectory tracking performance of the SP dynamic model, a Simulink model shown in Figure 10 is developed.
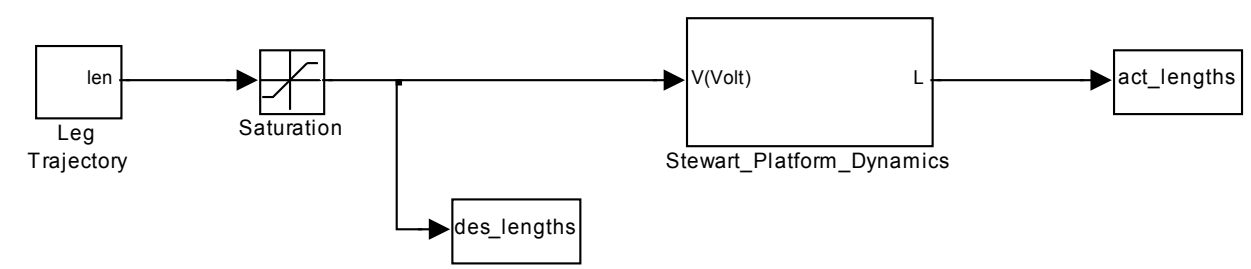

Fig. 10. Simulink model of the SP manipulator

In the figure, the reference lengths of the legs are limited between -25 mm and 25 mm with saturation block. The"*Stewart_Platform_Dynamics*" block computes the dynamic equations of the SP manipulator and outputs the actual lengths of the legs.

The attachment points GT_i and B_i on the moving and base platform, respectively are given in Table 1 and Table 2.

	GT_1 (m)	GT_2 (m)	GT_3 (m)	GT_4 (m)	GT_5 (m)	GT_6 (m)
X	0.0641	0.0641	0.0278	-0.0919	-0.0919	0.0278
Y	-0.0691	0.0691	0.0901	0.0209	-0.0209	-0.0901
Z	0	0	0	0	0	0

Table 1. Attachment point on the moving platform

	B_1 (m)	B_2 (m)	B_3 (m)	B_4 (m)	B_5 (m)	B_6 (m)
x	0.1451	0.1451	-0.0544	-0.0906	-0.0906	-0.0544
y	-0.0209	0.0209	0.1361	0.1152	-0.1152	-0.1361
z	0	0	0	0	0	0

Table 2. Attachment point on the base platform

Also, the system constants are given in Table 3.

Parameter	Value
m_{up}	1.1324 (Kg)
m_1	0.4279 (Kg)
m_2	0.1228 (Kg)
l_1	0.22 (m)
l_2	0.05 (m)
r_p	0.18867975191 (m)
r_{base}	0.29326616983 (m)
$I_{(mf)}$	$\begin{bmatrix} 0.0025 & 0 & 0 \\ 0 & 0.0025 & 0 \\ 0 & 0 & 0.005 \end{bmatrix} Kg.m^2$

Table 3. SP constants

The constants of the motor used in the SP manipulator are given in Table 4.

Parameter	Value
R	7.10 (ohm)
L	265e-6 (H)
K_b	2.730e-3 (V/rpm)
K_t	26.10e-3 (Nm/A)
n	1 (Rad/rad)
J_m	0.58e-6 (Kg.m²)
J_s	0.002091e-3 (Kg.m²)
b_m	0.0016430e-3 (N.s/rad)
b_s	0.11796e-3 (N.s/rad)
P	0.001 (m)

Table 4. SP motor constants

4.2 Dynamic simulations and experimental results

In this subsection, the effectiveness and the validation of the dynamic models of the SP manipulator with the actuator dynamics were investigated. In order to compare the experimental results with the simulation results, three trajectory tracking experiments were conducted. Also, the dynamic models obtained with two different Jacobian matrices (J_A and J_B) are examined. In all experiments, SP was worked in open-loop. In the first experiments, the translation motion along z-axis was applied to the SP system.

$$x(t) = 0 \qquad\qquad \alpha(t) = 0$$

$$y(t) = 0 \qquad\qquad \beta(t) = 0 \qquad\qquad (67)$$

$$z(t) = 0.25 + 10\sin(\pi t) \qquad \gamma(t) = 0$$

Figure 11 shows the reference lengths of the legs, the actual lengths from the encoder and the lengths predicted by the dynamic equations of the SP manipulator with two different Jacobian J_A (Sim-A) and J_B (Sim-B).
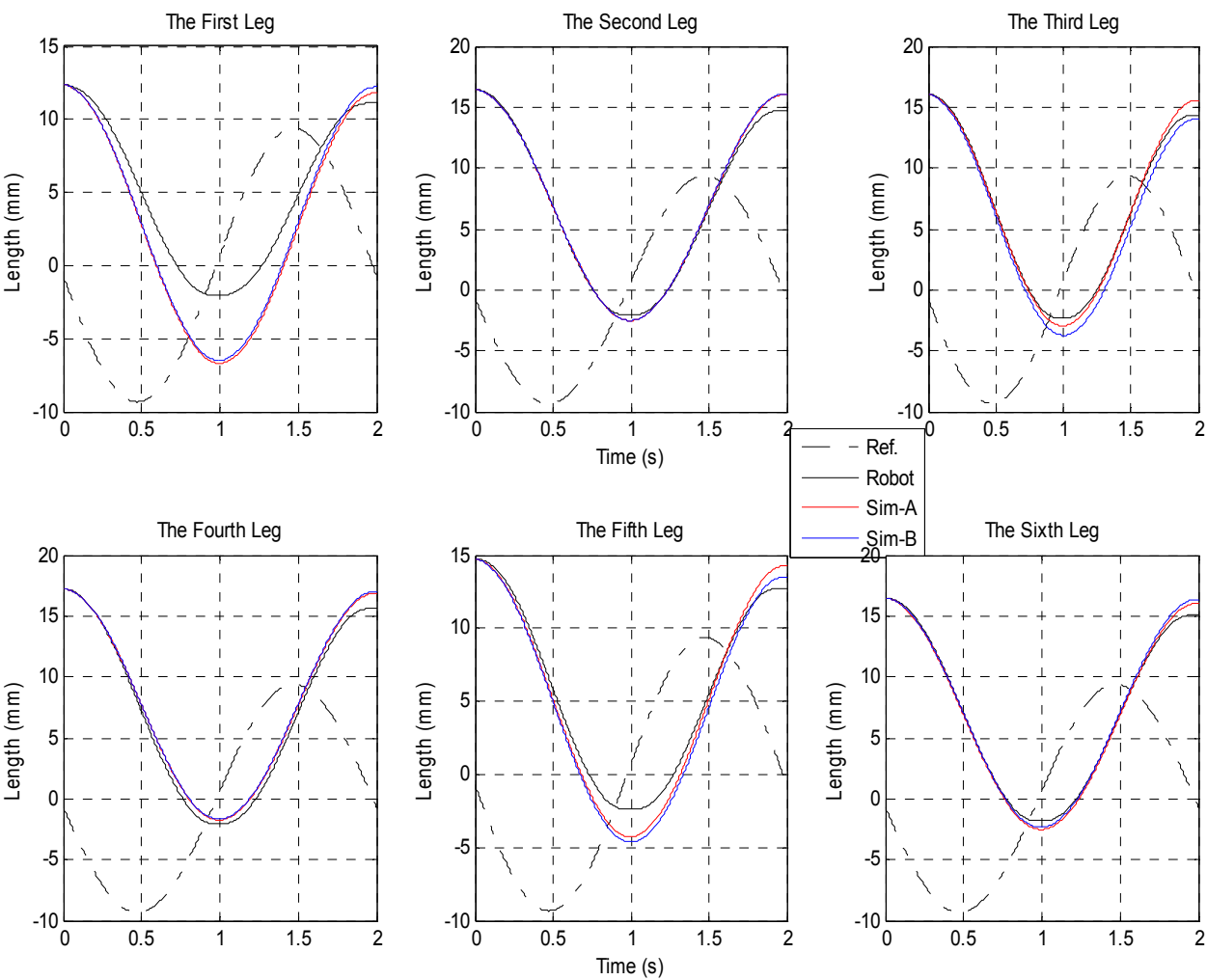

Fig. 11. Comparison of simulation results (red and blue) and experimental results (black) for the first experiment

Response of two dynamic simulation models (Sim-A and Sim-B) is almost same. But, it is observed that the *Sim-A* shows better performance than the *Sim-B* for this trajectory. Also, simulation and experimental results are very close to each other.

The second experiment, both translational and rotational motion along all axes (x,y,z) was applied to the SP system. The trajectory is defined in Equation 68. The experimental and simulation results for this trajectory are shown in Figure 12.
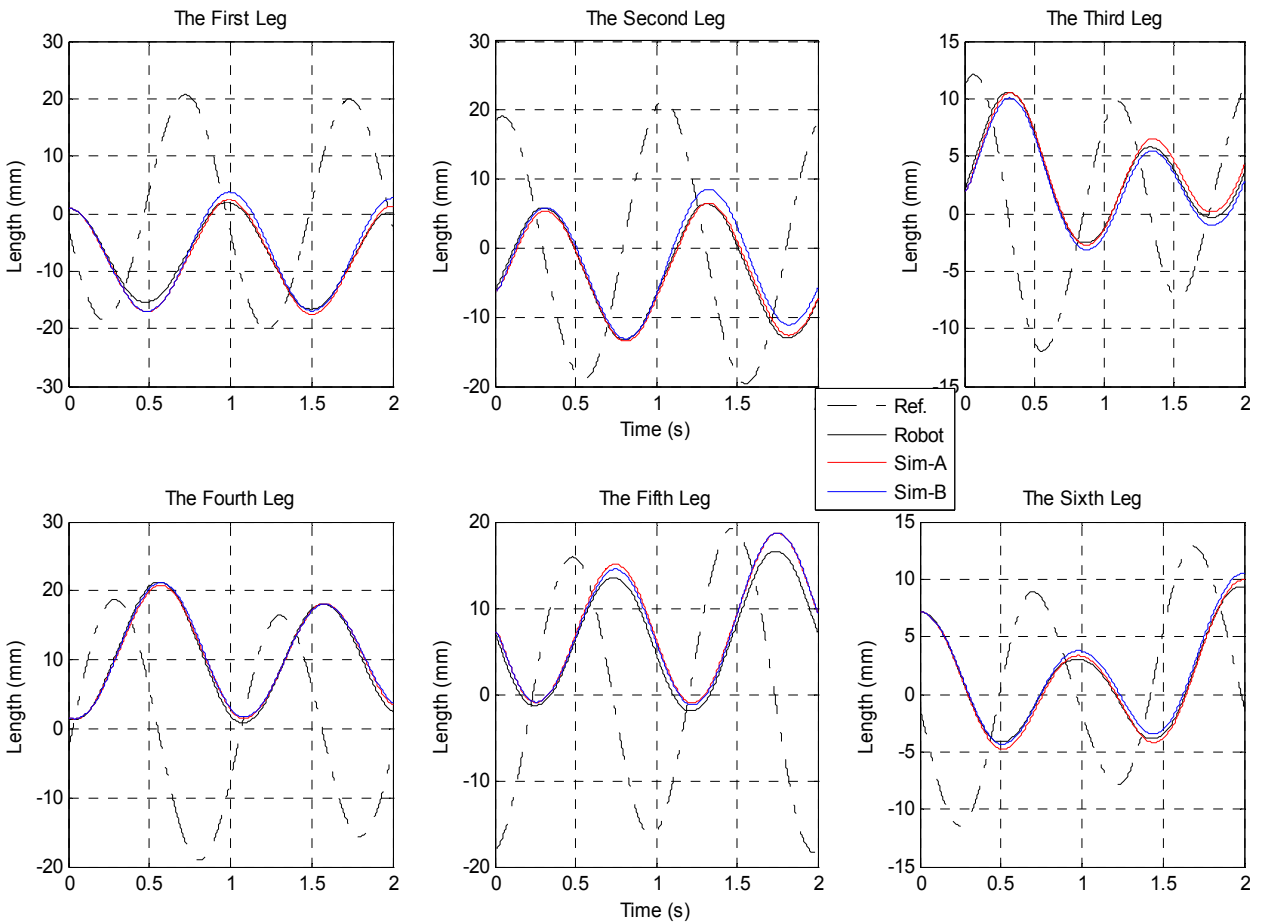
Fig. 12. Comparison of simulation results (red and blue) and experimental results (black) for the second experiment

$$x(t) = 5\sin(\pi t) \qquad\qquad \alpha(t) = 10\cos(2\pi t)$$

$$y(t) = 5\cos(\pi t) \qquad\qquad \beta(t) = 10\sin(2\pi t) \qquad (68)$$

$$z(t) = 0.25 + \sin(\pi t) \qquad\qquad \gamma(t) = 10\cos(2\pi t)$$

As can be shown in the figure, the dynamic model (red) has better performance compared to other (blue). There is good match between the simulation and experimental results.

In the last experiment, the fast translational and rotational motion along all axes (x,y,z) was conducted. The trajectory is given below.

$$x(t) = 10\sin(2\pi t) \qquad\qquad \alpha(t) = 5\cos(4\pi t)$$

$$y(t) = 10\cos(3\pi t) \qquad\qquad \beta(t) = 5\sin(5\pi t) \qquad (69)$$

$$z(t) = 0.25 + 3\sin(\pi t) \qquad\qquad \gamma(t) = 5\cos(3\pi t)$$

Figure 13 illustrates the results obtained from dynamic models and experimental results for this trajectory. In accordance with the results shown in Figure 13, the relative small deviations between the models and the experimental data are occurred. However, the obtained dynamic models can track the high frequency reference trajectory.
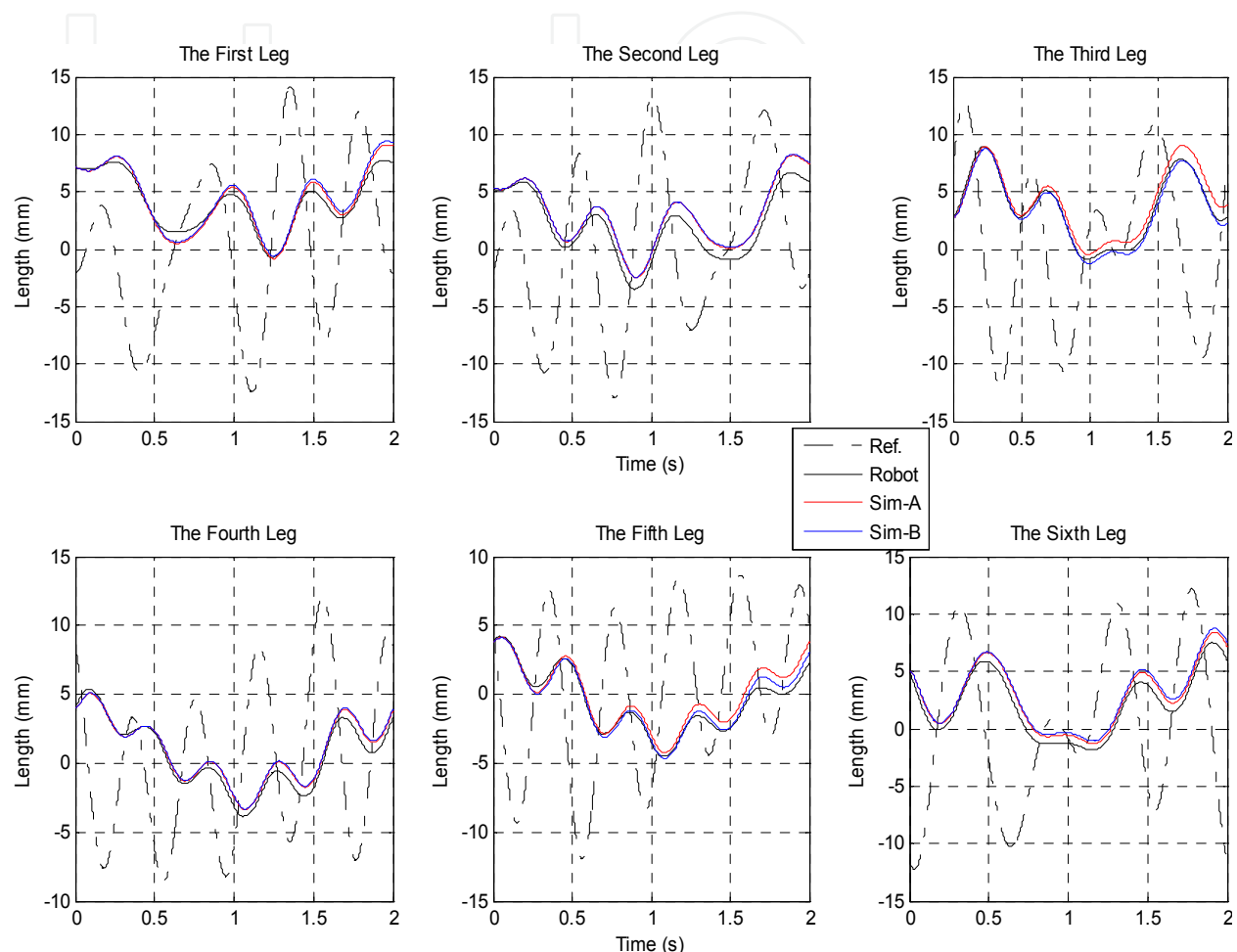

Fig. 13. Comparison of simulation results (red and blue) and experimental results (black) for the third experiment

The errors between simulation and experimental results were computed for all experiments. The cost function for the modeling error is defined as

$$E = \frac{1}{N}\sum_{i=1}^{N}|e_1(i)| + |e_2(i)| + |e_3(i)| + |e_4(i)| + |e_5(i)| + |e_6(i)| \tag{70}$$

where $e_1(i)...e_6(i)$ are the trajectory errors of ith sample obtained from difference between the experimental and the simulation results and N is the number of sample.

Table 5 gives the cost function values obtained from the two different dynamic models.

The two dynamic models of the SP manipulator using J_A and J_B exhibit very good performance in terms of model accuracy. Performance of the dynamic model using J_A is better than which of other model.

Experiment	Sim-A	Sim-B
1-EXP(z)	4.4337	5.0121
2-EXP(x,y,z,α,β,γ)	4.5389	4.5877
3-EXP(x,y,z,α,β,γ)	3.6470	3.3697

Table 5. The cost function values for the two different dynamic models

5. Conclusion

In this paper, closed-form dynamic equations of the SP manipulator with the actuator dynamics were derived using Lagrangian method. A computational highly efficient method was developed for the explicit dynamic equations. Besides, two simple methods for the calculation of the Jacobian matrix of SP were proposed. Two dynamic models of the SP were obtained using these Jacobian matrices. Two SP models were simulated in a MATLAB-Simulink. In order to verify the simulation results, three experiments were conducted. Considering all of the results, there is very good agreement between the experiments and the simulations. Modeling errors for each experiment were computed. Based on the modeling error, modeling accuracy of the developed models is very high. Thus, the verified model of the SP can be used for control and design purposes. Especially, a model based controller needs the verified model.

6. Acknowledgment

7. References

Abdellatif, H. & Heimann, B. (2009). Computational efficient inverse dynamics of 6-DOF fully parallel manipulators by using the Lagrangian formalism. *Mechanism and Machine Theory*, 44, pp. (192-207)

Beji, L. & Pascal, M. (1999). The Kinematics and the Full Minimal Dynamic Model of a 6-DOF Parallel Robot Manipulator. *Nonlinear Dynamics*, 18, pp. (339-356)

Bonev, I. A., & Ryu, J. A. (2000). New method for solving the direct kinematics of general 6-6 Stewart platforms using three linear extra sensors. *Mechanism and Machine Theory*, 35, pp. (423–436)

Carvalho, J. & Ceccarelli, M. (2001). A Closed-Form Formulation for the Inverse Dynamics of a Cassino Parallel Manipulator. *Multibody System Dynamics*, Vol. 5, pp. (185–210)

Dasgupta, B. & Mruthyunjaya, T. S. (1998). Closed-Form Dynamic Equations Of The General Stewart Platform Through The Newton-Euler. *Mechanism and Machine Theory*, 33 (7), pp. (993-1012)

Do, W. & Yang, D. (1988). Inverse Dynamic Analysis and Simulation of a Platform Type of Robot. *Journal of Robotic Systems*, Vol. 5, pp. (209-227)

Gallardo, J.; Rico, J.M.; Frisoli, A.; Checcacci, D.; Bergamasco, M. (2003). Dynamics of parallel manipulators by means of screw theory. *Mechanism and Machine Theory*, 38, pp. (1113–1131)

Geike, T. & McPhee J. (2003). Inverse dynamic analysis of parallel manipulators with full mobility. *Mechanism andMachine Theory*, 38, pp. (549–562)

Gregório, R. & Parenti-Castelli, V. (2004). Dynamics of a Class of Parallel Wrists. *Journal of Mechanical Design*, Vol. 126, pp. (436-441)

Guo, H. & Li, H. (2006). Dynamic analysis and simulation of a six degree of freedom Stewart platform manipulator. Proceedings of the Institution of Mechanical Engineers, Part C: *Journal of Mechanical Engineering Science*, Vol. 220, pp. (61-72)

Harib , K.; Srinivasan, K. (2003). Kinematic and dynamic analysis of Stewart platform-based machine tool structures, *Robotica*, 21(5), pp. (541–554)

Khalil W, Ibrahim O. (2007). General solution for the dynamic modelling of parallel robots.*J Intell Robot Systems,* 49, pp. (19-37)

Lebret G.; Liu K.; Lewis F. L. (1993). Dynamic analysis and control of a Stewart platform manipulator. *Journal of Robotic System*, 10, pp. (629-655)

Lee, K & Shah, D.K. (1988). Dynamical Analysis of a Three-Degrees-of-Freedom In-Parallel Actuated Manipulator. *IEEE Journal of Robotics and Automation*, 4(3).

Lin, J. & Chen, C.W. (2008). Computer-aided-symbolic dynamic modeling for Stewart-platform manipulator.*Robitica*, 27 (3), pp. (331-341)

Liu, K.; Lewis, F. L.; Lebret, G.; Taylor, D. (1993). The singularities and dynamics of a Stewart platform manipulator. *J. Intell. Robot.* Syst., 8, pp. (287–308)

Liu, M.J.; Li, C.X.; Li, C.N., 2000. Dynamics analysis of the Gough-Stewart platform manipulator. *IEEE Trans. Robot. Automat.*, 16 (1), pp. (94-98)

Meng, Q.; Zhang, T.; He, J-F.; Song, J-Y.; Han, J-W.(2010). Dynamic modeling of a 6-degree-of-freedom Stewart platform driven by a permanent magnet synchronous motor. *Journal of Zhejiang University-SCIENCE C (Computers & Electronics)*, 11(10), pp. (751-761)

Merlet, J.P. (1999). *Parallel Robots*, Kluwer Academic Publishers.

Merlet, J. P. (2004). Solving the forward kinematics of a Gough-type parallel manipulator with internal analysis. *International Journal of Robotics Research*, 23(3), pp. (221–235)

Reboulet, C. & Berthomieu, T. (1991). Dynamic Models of a Six Degree of Freedom Parallel Manipulators. *Proceedings of the IEEE International Conference on Robotics and Automation*, pp. (1153-1157)

Riebe, S. & Ulbrich, H. (2003). Modelling and online computation of the dynamics of a parallel kinematic with six degrees-of-freedom. *Arch ApplMech*, 72, pp. (817–29)

Staicu, S. & Zhang, D. (2008). A novel dynamic modelling approach for parallel mechanisms analysis. *Robot ComputIntegrManufact*, 24, pp. (167–172)

Stewart, D. (1965). A Platform with Six Degrees of Freedom, *Proceedings of the Institute of Mechanical Engineering*, Vol. 180, Part 1, No. 5, pp. (371-386)

Tsai L-W. (2000). Solving the inverse dynamics of Stewart–Gough manipulator by the principle of virtual work. *J Mech Des*, 122, pp. (3–9)

Wang, J. & Gosselin, C. (1998). A New Approach for the Dynamic Analysis of Parallel Manipulators. *Multibody System Dynamics*, 2, pp. (317-334)

Wang , Y. (2007). A direct numerical solution to forward kinematics of general Stewart–Gough platforms, *Robotica*, 25(1), pp. (121–128)
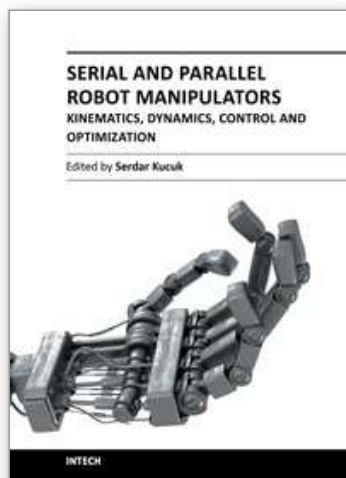
Serial and Parallel Robot Manipulators - Kinematics, Dynamics, Control and Optimization
Edited by Dr. Serdar Kucuk

The robotics is an important part of modern engineering and is related to a group of branches such as electric & electronics, computer, mathematics and mechanism design. The interest in robotics has been steadily increasing during the last decades. This concern has directly impacted the development of the novel theoretical research areas and products. This new book provides information about fundamental topics of serial and parallel manipulators such as kinematics & dynamics modeling, optimization, control algorithms and design strategies. I would like to thank all authors who have contributed the book chapters with their valuable novel ideas and current developments.

How to reference

In order to correctly reference this scholarly work, feel free to copy and paste the following:

Zafer Bingul and Oguzhan Karahan (2012). Dynamic Modeling and Simulation of Stewart Platform, Serial and Parallel Robot Manipulators - Kinematics, Dynamics, Control and Optimization, Dr. Serdar Kucuk (Ed.), ISBN: 978-953-51-0437-7, InTech, Available from: http://www.intechopen.com/books/serial-and-parallel-robot-manipulators-kinematics-dynamics-control-and-optimization/dynamic-modelling-of-stewart-platform

INTECH
open science | open minds